J Porous Mater (2013) 20:799–807
DOI 10.1007/s10934-012-9655-1

Development of ciprofloxacin hydrochloride loaded poly(ethylene glycol)/chitosan scaffold as wound dressing

Mukty Sinha · Rathindra M. Banik · Chandana Haldar · Pralay Maiti

Published online: 15 November 2012

Abstract A novel ciprofloxacin hydrochloride loaded chitosan/poly(ethylene glycol) (PEG) composite scaffold was developed for wound dressing application. PEG incorporation in chitosan scaffold showed enhanced loading up to 5.4 % and increased cumulative release of the drug up to 35 % as compared to pure chitosan scaffold (20 %). The drug loading and control release of the drug has been explained by the morphological features and drug–polymer/polymer–polymer interactions revealed by SEM, FTIR and DSC. Bacterial growth inhibition evaluation using *Escherichia coli, Pseudomonas aeruginosa* and *Staphylococcus aureus* confirmed the efficacy of released drug from the scaffolds (pure and PEG mixed chitosan). Swelling study, bacterial penetration, moisture vapour transmission rate, haematocompatibility and biodegradation profile supported the suitability of scaffold used as wound dressing materials. In-vivo study on mice finally validated the controlled rate of drug release showing the effectiveness of PEG incorporation into the scaffold for quicker and regulated wound healing.

Keywords Chitosan · Poly(ethylene glycol) · Wound dressing · Biodegradable polymers · Wound-healing

1 Introduction

Wound infection is among the major problems of wound care management. Oral route for antibiotic administration are widely used for treating such type of infections. But the route of administration has many side effects as high dose of drug is required to show the effect. Taking account of the shortcomings of oral route, topical method is tried to treat the infection by applying antibiotic loaded wound dressings [1]. Many polymeric materials are investigated for the purpose of wound dressing which include synthetic polymers like polyurethane, polyethylene, polycaprolactone, poly(lactic acid), polyacrylonitrile, poly(amino acid), silicone rubber. But there are few disadvantages of these synthetic polymers like toxicity, slow biodegradability and immune response [2]. To overcome these limitations, natural polymers such as chitin, chitosan, alginate, gelatine, collagen, etc. are used [3].

Chitosan (Cht) is easily processed into various forms which provide a wide variety of biomedical applications in tissue engineering, wound dressing, cancer drug delivery and drug targeting in the area of nanobiotechnology [4]. It is widely accepted for the applications due to biocompatibility, biodegradability and non-toxic nature. Chitosan wound dressing loaded with minocycline has shown faster healing properties. However, less drug loading efficiency

Electronic supplementary material The online version of this article (doi:10.1007/s10934-012-9655-1) contains supplementary material, which is available to authorized users.

M. Sinha · R. M. Banik (✉)
School of Biochemical Engineering, Indian Institute of Technology, Banaras Hindu University, Varanasi 221005, India
e-mail: rmbanik@gmail.com

M. Sinha
e-mail: mukty.rs.bce@itbhu.ac.in

C. Haldar
Department of Zoology, Faculty of Science, Banaras Hindu University, Varanasi 221005, India

P. Maiti
School of Material Science and Technology, Indian Institute of Technology, Banaras Hindu University, Varanasi 221005, India

of chitosan compelled to use combination of chitosan with other macromolecules [5]. Chitosan wound dressings either in pure or in blended form with poly(vinyl alcohol) have been reported in the literature [6]. Polyethylene glycol (PEG) is an excellent biocompatible and non-toxic polymer [7]. Having less mechanical strength, it is commonly blended or compounded with other polymers like alginate [8], collagen [9] applied in the field of controlled drug release. Among many methods for scaffold preparation, it is revealed that chitosan and its composite could easily be fabricated into porous three dimensional scaffolds using electrospinning, salt leaching, thermally induced phase separation and freeze drying techniques. But, freeze drying method is preferred over the others due to possibility for modulating microstructure, crystallinity and the most important for economic viability [10].

Fluoroquinolones are well-established broad spectrum antibiotics having potent bactericidal activity against most common pathogens which are prevalent at wound site such as *Staphylococcus aureus, Pseudomonas aeruginosa* etc. [11]. Among them, ciprofloxacin is one of the most widely used fluoroquinolones to treat a variety of bacterial infections [12]. Oral administration of ciprofloxacin is still available in market as conventional immediate-release tablets.

To our knowledge, this is the first report of ciprofloxacin loaded Cht–PEG composite scaffold for wound dressing purpose. The objective of the study was to develop antibiotic loaded wound dressing using chitosan–PEG scaffold and to investigate its effectiveness for wound healing. In the present work, biocompatible chitosan scaffold was developed by freeze gelation technique. Further, chitosan scaffold was modified with PEG for faster and regulated drug release requirements. The comparative release rates have been examined through interaction between drug and scaffold matrix. Various physicochemical studies were performed namely, bacterial penetration, swelling study, mechanical strength and moisture vapour transmission rate for confirming its suitability as wound dressing material. Finally, haematocompatibility and in vivo study was performed to demonstrate the efficacy of the developed scaffold for the desired purpose evidenced by wound morphology and cell growth through histological studies.

2 Materials and methods

2.1 Materials

Chitosan was obtained from Marine Chemicals, Chennai, India; the degree of deacetylation (DD) 85 %. Polyethylene glycol 4000 and ethanol of high purity grade was obtained from Merck, Mumbai, India. Ciprofloxacin hydrochloride was gift sample obtained from Elcon Drugs and Formulation Ltd., Jaipur, India. *Escherichia coli* MTCC 739, *Staphylococcus aureus* MTCC 96 were procured from Microbial Type Culture Collection (MTCC), Chandigarh, India and *Pseudomonas aeruginosa* NCIM 2948 was purchased from National Chemical Laboratory (NCL), Pune, India, respectively.

2.2 Preparation of polymeric scaffold

Polymeric scaffolds were prepared by freeze gelation method [13]. Precisely, 2 g chitosan was solubilized in 100 ml of 0.1 N acetic acid under stirring at room temperature. The resulting polymeric solution was centrifuged for 15 min at 3,000 rpm for degassing. The degassed solution was poured into glass petridish and kept in deep freezer (Cryo scientific, URC-V, 500-2) at −20 °C for 24 h. Sodium hydroxide (1 N) was added to the frozen sample in the petridish. Then, the three dimensional structure formed due to phase separation was washed with absolute ethanol and finally lyophilized.

Later, the composite chitosan–PEG scaffold was prepared by blending PEG in different proportions to the initial chitosan solution and using above mentioned steps. Antibiotic loaded scaffolds were prepared by adding CPR into the polymeric solution at initial step of scaffold preparation.

2.3 Release study

In-vitro drug release study was performed in phosphate buffered saline (PBS) at pH ∼7.4. The antibiotic containing scaffold of unit dimension (1 cm^2) was put into PBS and incubated in a shaker at 35 °C at 50 rpm. At predetermined time intervals, 2 ml samples were withdrawn and replaced with same amount of fresh buffer. Concentration of CPR in the samples was measured by taking absorbance at 277 nm using UV–Vis Spectrophotometer (Shimadzu, 1700).

2.4 Characterization

FTIR spectroscopy (*Shimadzu, 8400S*) was used to observe polymer–polymer/antibiotic–polymer interactions. Dried scaffold samples were mixed with dry KBr powder and pressed to form a pellet. The solid pellet was placed in magnetic holder and data was recorded from 1,000 to 4,000 cm^{-1}.

The surface morphology of the scaffolds (1 cm^2) was examined using scanning electron microscope (*JEOL JSM 5600*) to observe the micro porous structures of the scaffold.

Differential scanning calorimeter (*Mettler–Toledo*) was used to study the transition temperature of chitosan and the Cht–PEG composites. The specimens were placed in aluminium pans and heated from 40 to 240 °C at a heating rate of 20 °C/min under a nitrogen atmosphere.

X-ray diffraction (XRD) pattern of the sample was recorded on an *X*-ray diffractometer (*Bruker D8 Advance X-ray diffractometer*) from 5° to 50° at room temperature at 5°/min scanning rate.

Tensile properties of the samples were determined in dry state using Universal Testing Machine (*Instron 3369, UK*) tensile tester at a strain rate of 5 mm min^{-1} at 25 °C. Dumbbell shaped strips of 3 mm width were cut and thickness measured using a micrometer. Mean of 3 samples were computed to estimate error.

2.5 Bacterial growth evaluation

The evaluation was done by turbidimetric method and measurement of zone of inhibition. In turbidimetric method, *E. coli* was grown in nutrient broth (Hi-media, India) for 24 h. The bacterial solution was standardized to an absorbance value between 1.0 and 0.2 at 625 nm using 5 ml aliquot for experiment. Scaffolds (1 cm^2) with or without antibiotic were added to each aliquot. All tested solutions were incubated at 37 °C with constant shaking and the absorbance at 625 nm was monitored after 24 h of incubation. The percentage of bacterial inhibition was calculated by the following equation:

$$\text{Bacterial inhibition}\,(\%) = \frac{I_c - I_s}{I_c} \times 100 \quad (1)$$

where, I_c and I_s are the absorbance of the control (scaffolds without antibiotic) and test bacterial solution with medicated scaffold, respectively. The significance (*P*) for all the tests was set at $P < 0.05$, and all the data were expressed as the mean ± S.D ($n = 3$). Additionally, a second viability test involved the use of bacterial colony formation and measurement of zone of inhibition. In this test, scaffolds sections (1 cm^2) of varying formulations (i.e., Cht and Cht–PEG scaffold with and without CPR) were incubated at 37 °C for 24 h on agar plates for diffusion of CPR from the scaffold into the agar (in case of medicated scaffolds). 10 µl aliquot of *S. aureus, P. aeruginosa* and *E. coli* were spread onto the plate, and the plates were incubated overnight at 37 °C. Bacterial growth was visualized directly on the plate and the zone of inhibition was measured [14].

2.6 Swelling study

Predetermined weights of 1 cm^2 scaffolds were immersed in phosphate buffered saline (PBS) and distilled water. After immersing for 1, 2, 3 and 7 days at 37 °C, the swollen scaffolds were removed from the water or PBS, gently blotted with filter paper to remove surface liquid and immediately weighed.

$$\text{Swelling}\,(\%) = \frac{(W_t) - (W_o)}{(W_o)} \times 100 \quad (2)$$

where, W_t and W_o are final and initial weight of the scaffolds, respectively [15].

2.7 Water vapour transmission rate (WVTR)

The water vapour transmission rate was calculated using the *JIS 1099A* standard method [11]. A round piece of scaffold was mounted on the mouth of a cup (4 cm dia) containing 50 g of $CaCl_2$ and placed in an incubator of 90 % RH at 40 °C. The water vapour transmission rate (WVTR) was determined as follows:

$$\text{WVTR}\,(g/m^2 - \text{day}) = \frac{(W_2) - (W_1)}{s} \times 24 \quad (3)$$

where, W_1 and W_2 are the weights of the whole cup at the first and second hours, respectively, and *S* was the transmitting area of the sample.

2.8 Bacterial penetration study

5 µl Suspension of *E. coli* in saline phosphate buffer pH 7.4 was dropped above the centre of the upper surface of scaffold discs (1 cm^2) previously placed on sterile nutrient agar culture medium in petridishes. The suspension was carefully deposited on the disc without contaminating the agar medium. The petridishes were then incubated for 24 h at 30 °C and the growth of bacteria on the surface of the agar media was visually inspected [16]. The penetration of bacteria through the scaffolds was verified by colonies that may grow on the agar surrounding the discs after penetrating the scaffold.

2.9 In-vitro biodegradation of wound dressing

The biodegradation study was conducted in vitro by incubating the scaffolds of 1 cm^2 in phosphate buffered saline (pH ~7.4) with 500 U/C.C. of lysozyme concentration and kept at 37 °C. At predetermined time intervals, the concentration of remaining lysozyme and reducing sugar was calculated in the buffer solution using Bradford and DNS method, respectively. The remaining weight of the complex after the enzymatic degradation was calculated using the following equation:

$$\text{Weight remaining}\,(\%) = (W_{after}/W_{before}) \times 100\% \quad (4)$$

where, W_{before} and W_{after} were the dry weights of the material before and after degradation, respectively.

2.10 Haematocompatibility

Haematocompatibility test was performed by reported method [17]. Heparinized polymeric scaffolds were cut into small pieces (1 cm^2) and ACD (acid citrate dextrose) human blood (0.2 ml) was added to each sample. After a predetermined time period, 4 ml of saline water added to each sample to stop hemolysis and the samples were kept for 1 h. Positive (PC) and negative controls (NC) were prepared by adding 0.2 ml of human blood to 4 ml of distilled and saline water, respectively. All the samples were centrifuged and absorbance of the supernatant was measured at 545 nm to calculate the percent of hemolysis as follows:

$$\%\ \text{Haemolysis} = \frac{OD_s - OD_{NC}}{OD_{PC} - OD_{NC}} \times 100 \quad (5)$$

where, OD_s, OD_{NC} and OD_{PC} are optical density of sample, negative and positive control, respectively.

2.11 In-vivo wound healing test

Albino male mice (40 ± 5 g) were taken as model animal for the experiment. To carry out the in vivo experiments permission was taken from Central Animal Ethical Committee of the University (*Dean/10-11/190*). Experiment was designed to minimize the error by taking 5 male mice for each dressing (including control) at 5 sampling time point. The experiment was performed under anesthesia using anesthetic ether. Dorsal hair of each animal was shaved followed by the creation of full thickness wound areas (2 mm^2) by excising the dorsum, and the area was sterilized wiping with cotton soaked in 70 % alcohol. Wounds were covered with Cht–CPR, Cht–PEG–CPR scaffolds and control having open wound. All wound dressing materials were fixed with an elastic adhesive bandage. Treated mice were placed in individual cages and wounds healing process were observed at the 3rd, 6th, 9th, 14th and 21st postoperative days. The animals were maintained on ad libitum diet of tap water and standard laboratory mice feed until sacrifice of the animal. Following the operation, each wound size was measured and image was taken (Olympus).

2.12 Histological study

The wounded area of skin containing dermis and hypodermis was crossly trimmed. All trimmed skins were fixed in 10 % neutral buffered formalin. After paraffin embedding, 5 μm sections were prepared using Microtome, Leica, *USA*. Representative sections were stained with hematoxylin and eosin (HE) for microscopic examination [18].

3 Results and discussion

3.1 Preparation of chitosan scaffold

Three dimensional porous chitosan scaffolds were prepared by freeze gelation method using sodium hydroxide (NaOH) as gelling agent [19]. It has been proven that gelation using NaOH provides some haemostatic effect to the scaffold [20]. Phase separation of water and polymer molecules takes place during freezing due to formation of ice crystals at −20 °C and subsequently, melting of ice at ambient condition generates pores in the scaffolds. Gelling of the polymer was performed using NaOH for the structural rigidity of the scaffold. The chitosan scaffolds formed were whitish against the yellowish powder of pure chitosan.

3.2 Effect of additive on antibiotic release

The influence of different concentrations of chitosan (1, 2 and 3 wt%) in the antibiotic loaded scaffold on the release in phosphate buffer saline, pH ~7.4 have been studied previously by [13]. From the previously reported study, 2 wt% chitosan concentration was chosen for further modification to improve drug loading efficiency. Percent antibiotic loading depicts highest loading (6.4 %) in Cht–PEG blended scaffold in 1:1 ratio compared to 1:2 and 2:1 ratio. Moreover, the addition of poly(ethylene glycol) (PEG) to 2 wt% chitosan scaffold (1:1) has remarkably enhanced the antibiotic release compared with pure chitosan scaffolds as shown in Fig. 1. The antibiotic release was 30 % in modified scaffold in comparison to only 20 % in pure chitosan scaffold. Hence, significantly higher cumulative release was seen from composite scaffold as

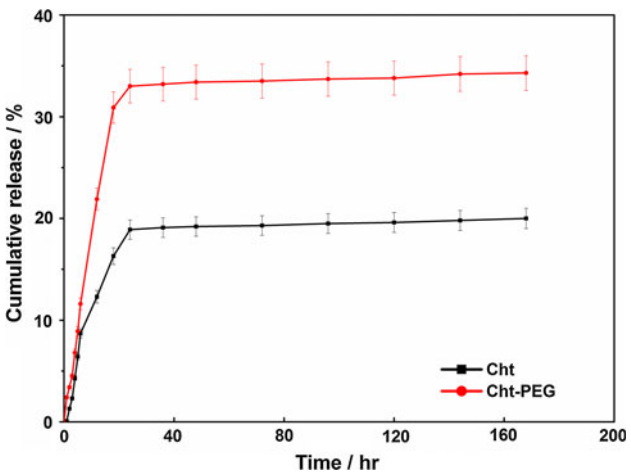

Fig. 1 Release of antibiotic from different scaffolds with polymeric concentration of 2 wt% chitosan and PEG modified chitosan scaffold (1:1)

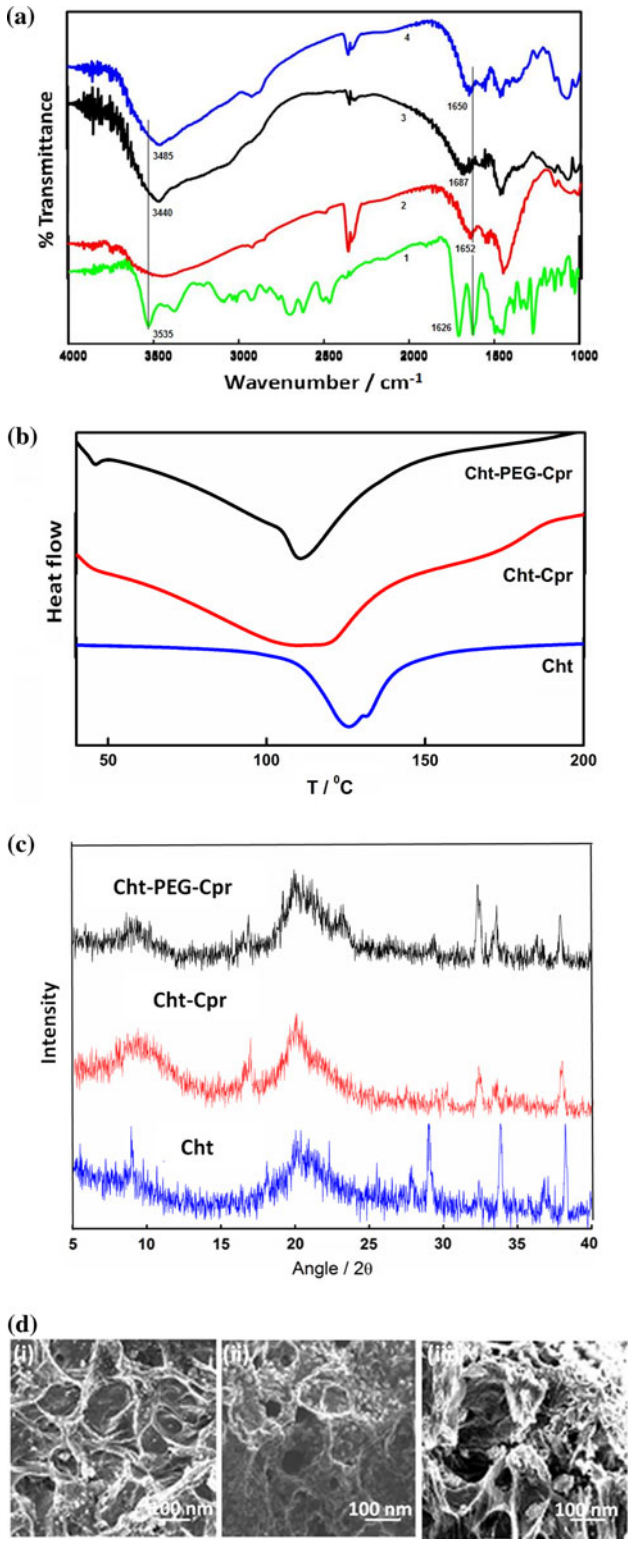

Fig. 2 **a** FTIR spectra of Ciprofloxacin (*1*), chitosan (*2*), Chitosan having ciprofloxacin (*3*) and, chitosan mixed with PEG (1:1) with drug (*4*); **b** differential scanning colorimetry of pure chitosan, chitosan with antibiotic and CPR loaded chitosan scaffold blended with PEG; **c** XRD patterns of scaffolds of chitosan (Cht-2), chitosan with antibiotic and chitosan modified with PEG and CPR; **d** scanning electron microscopy of different scaffold *i* Cht, *ii* Cht–CPR, and *iii* Cht–PEG–CPR

compared to previously reported pure chitosan scaffold. Coleman & Painter showed higher cumulative drug release with increasing concentration of PEG using chitosan in the film form [21]. However, this work demonstrates faster release of antibiotic by incorporating specified amount of PEG (ratio 1:1) in the antibiotic-loaded scaffolds.

3.3 Interactions of the scaffolds

To investigate the nature and extent of interaction, FTIR spectra of Cht, Cht–CPR and Cht–PEG–CPR was studied. The characteristic peaks of chitosan due to –OH/–NH_2 stretching, –C(=O)– stretching and –NH_2 bending are located at 3,474, 1,652 and 1,563 cm^{-1}, respectively as shown in Fig. 2a [22]. On the other hand, the main peak for pure ciprofloxacin at 3,535 and 1,710 cm^{-1} appears for –OH/–NH stretching and carbonyl stretching, respectively [23]. Significant shift of –OH/–NH stretching to 3,440 cm^{-1} from 3,474 cm^{-1} has been observed for antibiotic loaded scaffold indicating stronger interaction between the antibiotic and chitosan molecules in the scaffold presumably through hydrogen bonding. The overlapped band in the region of 3,200–3,700 cm^{-1}, which is assigned to the N–H and O–H stretching bands of chitosan component [20], clearly become sharper at 3,475 cm^{-1} due to interaction with the antibiotic. Further, the strong band at 1,687 cm^{-1} (shifted from 1,652 cm^{-1} which is of –C(=O)– stretching) also supports the intimate interaction between ciprofloxacin and chitosan in the scaffold. In both the cases, the interaction occurs through hydrogen bonding between carbonyl and –OH/–NH moieties from polymer and antibiotic. In case of Cht–PEG–CPR, –C(=O)– and –OH/–NH peaks have been shifted to 1,650 and 3,485 cm^{-1} upon addition of PEG in Cht–CPR scaffold suggesting the weakening of interaction between chitosan and ciprofloxacin as compared to pure scaffold while maintaining sufficient interaction revealed by the deviation from pure stretching frequencies. In the broad region of 3,200–3,700 cm^{-1}, the change of the slope of the overlapped band $\sim$3,500 cm^{-1} is a further indication of an increased intermolecular interaction. It is obvious that PEG is interactive with chitosan leading to weaken of the Cht–CPR binding and, thereby, facilitating the antibiotic release at a faster rate in presence of PEG in the scaffold. The N–H stretching mode has been used as a measure of intermolecular interaction and the subsequent miscibility [21].

The depression of phase transition temperature is a measure of interaction in the blended system. Figure 2b shows the DSC thermograms of pure chitosan and antibiotic loaded systems. The first order phase transition at 126 °C for pure chitosan corresponds to the loss of water from the scaffold. There is a significant reduction of

Table 1 Mechanical properties of pure chitosan and the blend (Cht–PEG) scaffold

Sample	Tensile strength (MPa)	% Strain	Young's modulus (MPa)
Cht 2 wt%	45 ± 5.2	89.2 ± 5.4	65 ± 11
Cht–PEG	12 ± 1.1	256 ± 40	1.6 ± 0.3

transition temperature for Cht–CPR blend (114 °C) as compared to pure chitosan (126 °C). The transition temperature further reduces in presence of PEG (108.5 °C) indicating even better interactions between chitosan and PEG which was estimated from FTIR studies as well.

The effect of intermolecular interactions on the crystallization behaviour of the Cht–PEG scaffold was studied by using XRD as shown in Fig. 2c. The *X*-ray diffraction patterns of the pure chitosan powder shows three characteristic peaks at 2Θ about 10.3°, 15.9°, and 20.18° which indicate a high degree of crystallinity as shown in the previous report [24]. The peak at 9.03° disappears in antibiotic loaded chitosan scaffold and an amorphous halo was seen at ~9°. Other major peaks of the pure scaffold at 29.05, 33.88 and 38.19° also get reduced/abolished in presence of CPR indicating greater interaction. Thus, FTIR, DSC and XRD studies have revealed the interactions between chitosan and the antibiotic and compares it with PEG loaded system as well strengthening the relative rate of antibiotic release in different systems based on their overall interactions.

From Table 1 chitosan scaffold of 2 wt% exhibited a tensile strength of 45 ± 5.2 MPa while the Cht–PEG blend scaffold had a value of 12 ± 1.1 MPa. The corresponding elongation was 89.2 ± 5.4 and 256 ± 40 %, respectively. The results confirmed that blending with PEG resulted in decrease in the tensile strength of chitosan. The modulus value of pure polymeric scaffold also significantly decreased on blending with PEG. Similar results were reported by Zhang et al. [25].

3.4 Morphological control of the modified scaffold

The microstructures of the Cht, Cht–PEG scaffolds with and without CPR were investigated by scanning electron microscopy and presented in Fig. 2d. Many white grains appear on the surface of CPR loaded scaffold presumably due to agglomeration caused by the presence of the antibiotic [Fig. 2d (ii)]. The surface of Cht–PEG scaffold was relatively more porous in comparison with pure chitosan scaffold having thinner fibrils [Fig. 2d (iii)] which explains higher CPR release rate in presence PEG as compared to relatively less porous antibiotic loaded chitosan scaffold. Microstructure analysis through SEM showed comparatively better pores distribution in the composite scaffold which supported the antibiotic release behaviour. Yang [12] showed decrease of porosity and swelling behaviour with increasing polymer concentration, which affected the cumulative drug release.

3.5 Antibacterial efficacy

Antibiotic incorporation in the formulation must be effective after getting released at the site. The clear solution using Cht–PEG scaffold as compared to turbid control solution has clearly been seen justifying the effectiveness of the released antibiotic in eradicating the bacterial population. Antibiotic loaded chitosan scaffold also exhibits inhibition but comparatively less than Cht–PEG system as indicated from the slight hazy solution (Supplementary Fig.1). The extent of effectiveness of released antibiotic from the scaffold is compared in Table 2, indicating the superiority of the antibiotic loaded Cht–PEG composite scaffold over pure chitosan scaffold in inhibiting the bacterial growth. The statement is also supported by the zone of inhibition results.

3.6 Biodegradation for antibiotic delivery

Figure 3a represents the gradual increasing tendency of total reduced sugar produced from Cht and Cht–PEG scaffolds after getting hydrolysed by enzyme with time. Simultaneously, weight of scaffold has reduced in the enzymatic media after reacting with chitosan scaffolds sample (Fig. 3b). The enzyme concentration, measured by Bradford method, also decreased implying its consumption by the scaffold for its degradation. Chitosan is polysaccharides and gets degraded into smaller reducing sugar unit by the action of lysozyme in animal system [26]. Hence, the increasing tendency of reducing sugar concentration and decreasing nature of remaining weight confirms the biodegradation of the scaffold in enzymatic media which definitely facilitates the antibiotic delivery at late stage.

Table 2 Bacterial growth evaluation of released drug from chitosan and Cht–PEG by turbidometric and zone of inhibition method

Sample	Bacterial inhibition (%) = $I_c - I_s / I_c \times 100$	Average zone of inhibition (cm)		
		E. coli	*P. aeruginosa*	*S. aureus*
Blank	29	0	0	0
Cht–Cpr	71.5	3	3.3	3.5
Cht–PEG–Cpr	87	3.5	3.7	3.8

I_c absorbance of control, I_s absorbance of sample taken at 660 nm; n = 3

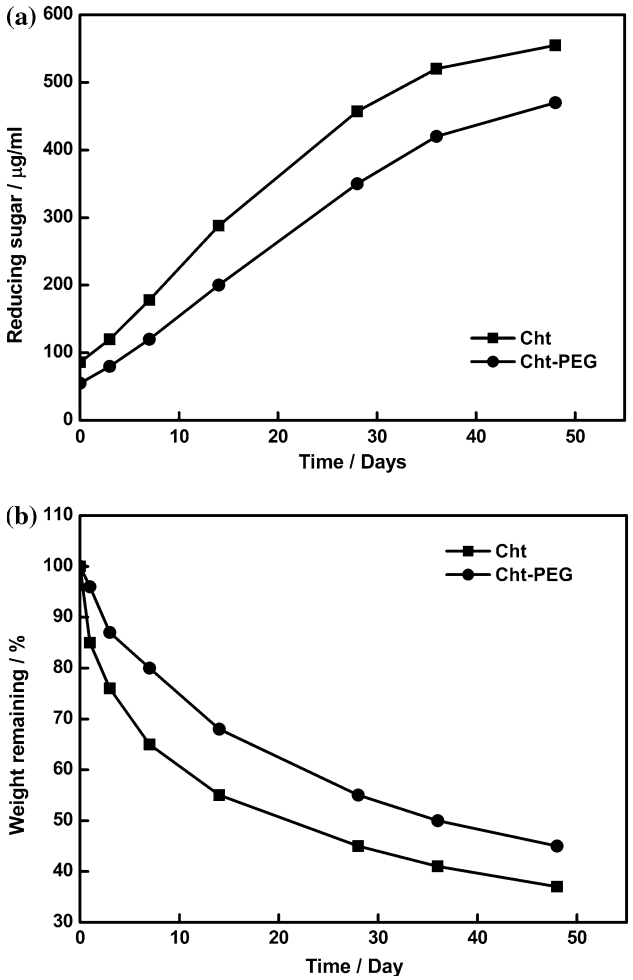

Fig. 3 Lysozymatic degradation of chitosan and Cht–PEG scaffold showing **a** increment in reducing sugar into the medium, and **b** decrease in scaffold weight with time

3.7 Physical properties of wound dressing

Swelling study shows the equilibrium water content/swelling ratio of films in different buffer (Supplementary Fig. 2). The study demonstrated effect of pH on chitosan swelling. As obvious from the results, swelling of the scaffold was highest in citrate buffer (pH ~4.5) and lowest in saline phosphate buffer (pH ~7.4). The possible reason lies on more solubility of chitosan in acidic pH owing to the presence of free amine groups. Interestingly, lower pH of infected wound facilitates faster swelling and, hence, more exudates would be replaced. As a result, spreading of infection would be inhibited and healing promoted.

One of the main functions of wound dressing membrane is to maintain moist environment at the wound/dressing interface. Table 3 shows WVTR of pure and blended chitosan scaffolds demonstrating increase in membrane permeability of the PEG modified scaffold as compared to pure chitosan. An ideal dressing should control the water loss/evaporation from a wound at an optimal rate. The rate is 204 g/m^2 per day for normal skin, which increase up to 5,138 g/m^2 per day for a granulating wound. It was recommended that a rate of 2,500 g/m^2 per day, being in the mid-range of loss rates from injured skin, would provide an adequate level of moisture without risking wound

Table 3 Water vapour transmission rate (WVTR) of various scaffolds

Sample	WVTR (g/m^2.day)	Hemolysis (%)	Bacterial penetration
Blank	4,026	2.10	Present
Cht	2,157	1.84	Absent
Cht–Cpr	2,174	1.93	Absent
Cht–PEG–Cpr	2,357	1.86	Absent

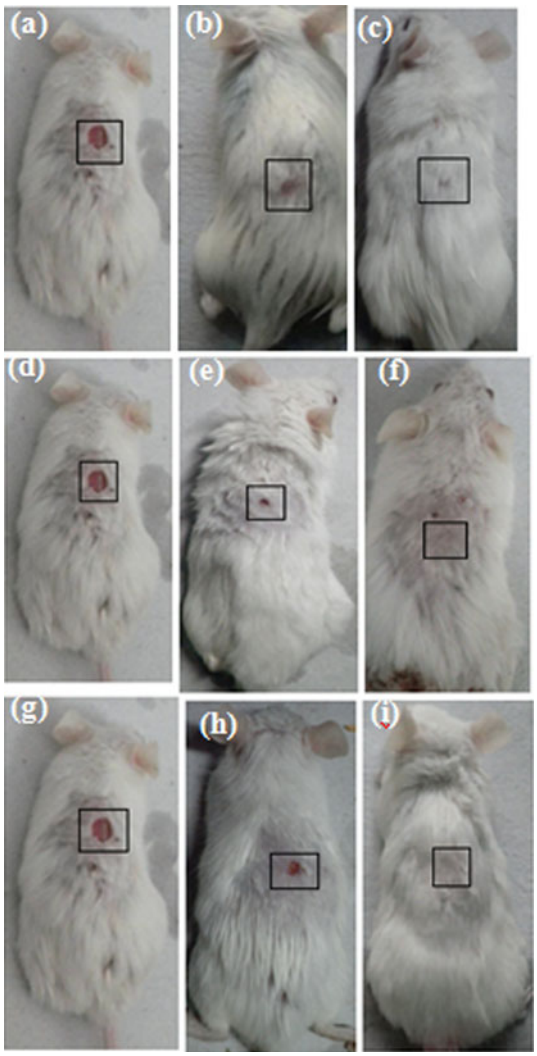

Fig. 4 Mice showing wound area without dressing (**a**–**c**): **a** 0 day, **b** 14 days, and **c** 21 days; using the dressing of chitosan and drug (**d**–**f**): **d** 0 day, **e** 9 days, **f** 14 days; and using Cht–PEG–CPR (**g**–**i**): **g** 0 day, **h** 6 days, **i** 9 days

dehydration. The enhanced porosity of sponge-like sublayers increases the adsorption of water vapour into the structure. Simultaneously, decreased thickness of dense skin layer also increases the diffusion of water molecules through the porous structure resulting in increased water vapour transmission rate (WVTR) [1]. The increase of the PEG modified chitosan permeability has proven the increase of the hydrophilicity of the membrane due to presence of amine groups which improves the swelling ratio and diminish the pore size. The reported WVTR for commercially used dressings are 480 and 1,040 g/m^2 per day for *Duoderm CGF* and Gauze, respectively, quite low as compared to this study [12].

Table 3 also shows the bacterial penetration through these scaffolds which confirms that bacteria cannot penetrate through the antibiotic loaded modified scaffold. The microporous structure of scaffolds which is in zig-zag form may slow down the movement the microorganisms. Moreover, antibiotic containing scaffolds are itself inhibitory for the penetration. Hemolysis of the blood is the problem associated with bio-incompatibility [27]. It is observed in Table 3 that hemolysis is less than 5 % in all the cases which is within the acceptable limit.

3.8 In-vivo antibiotic release study and the effect on cell growth

The scaffolds were applied over artificially created wound spots on the mice dorsum to examine the effect of the developed dressing on wound healing. The consequence of scaffolds composed of Cht–CPR and Cht–PEG–CPR is compared with control (without applying dressing) on various days of post operation as described in Fig. 4 showing macroscopic appearance (optical images) of the wounds. All mice were survived throughout the post-operative period until sacrifice without any evidence of necrosis. On 3rd day of post operation, little discrete inflammation was observed in all mice. A clean wound with pinkish colour was observed. On 6th day of post-operation, the control showed slight hemorrhage as secondary damage. On the contrary, the dressing hardly induced any hemorrhage. The relative size reduction of the wounds treated with various dressing materials is illustrated in Fig. 4. The chitosan membrane was found to adhere uniformly to the freshly excised wound surface and also adsorbed the exudates from the wound surface. On 14th postoperative day, the chitosan scaffold with antibiotic was no longer adhered to the wound as complete healing occurred (Fig. 4d–f). On the other hand, the majority of the wounds were completely healed in just 9 days of post-operation using Cht–PEG antibiotic loaded scaffold (Fig. 4g–i); whereas in the control and antibiotic loaded chitosan still had small opening seen with scar in the same period. Developed chitosan scaffolds blended with PEG attained uniform adherence to the wound surfaces throughout healing without any fluid accumulation. Song reported that PEG has cell adhesive property in addition to which is supported in present study [28]. In

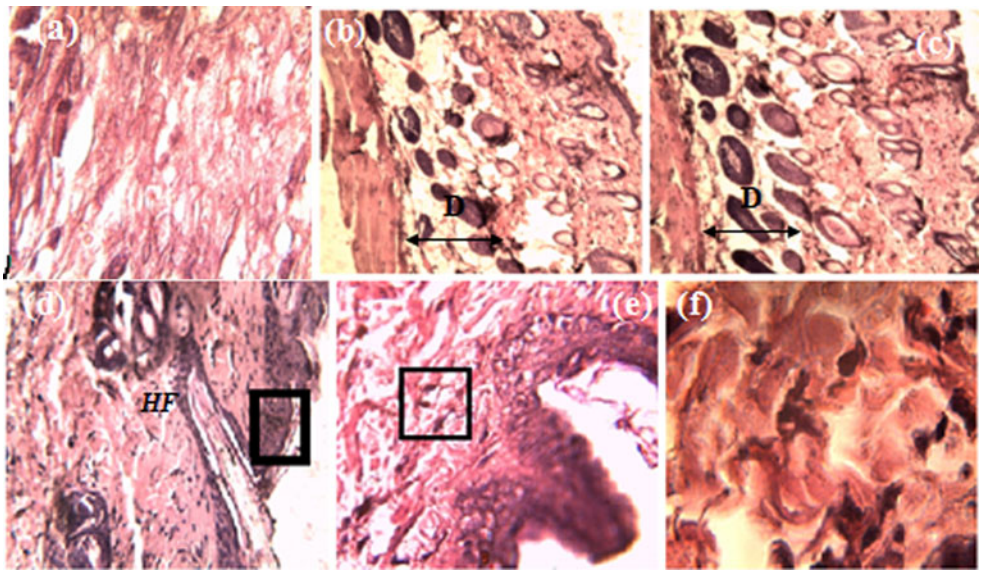

Fig. 5 Histological appearance of wound healing **a** first day, **b–f** 9th day of wound healing under different magnifications: **a** 10× showing only musculature; **b** 10× showing appearance of epithelial covering of tissues healed without dressing and cell arrangement in dermal area (*marked area*); **c** 10× showing appearance of epithelial covering of tissues healed using Cht–PEG–CPR and cell arrangement in dermal area (*marked area*); **d** 45× showing epithelium cell proliferation (*marked area*) and hair follicle (HF) in tissues healed using Cht–PEG–CPR; **e** 100× showing enlarged view of *marked area* in **d**, epidermal cell arrangement and collagen presence (*marked area*); and **f** 100× showing enlarged view of *marked area* in **e**, presence of collagen

addition, epithelialisation acceleration and keratinocyte migration occurred more easily in the mice models onto which dressing containing PEG was applied [5].

Wound healing was very slow in control system (without scaffold) completed in 21 days (Fig. 4a–c). Epithelialization of the wound was advanced but the dermis was still somewhat inflammatory in control mice. The chitosan-membrane treated wound had well organized epithelialization with a horny layer as covering. Wound was healed in control system around 21 days but still the epidermal layer was having an impression of wound. However, in case of Cht–PEG system wound was healed within 9 days as obvious from faster in vitro antibiotic release obtained from the drug release data (Fig. 1), while wound having CPR loaded chitosan was healed in longer period of 14 days.

Histological examination of the wounds was performed to observe the cell growth during healing process. Only muscles, without any dermis and epidermis, were observed in the initial phase (Fig. 5a). The wound covered with chitosan scaffolds showed the epithelialization process on day 3 and the dermis was rich in polynuclear and macrophage inflammatory cells. The extent of infiltration of polynuclear and macrophage inflammatory cells being more in number for wound covered with sponge-like Cht–PEG wound dressing than the control. The deposition of newly synthesized collagen in the wound is well organized and oriented along the skin surface, suggesting a perfect repairing of the damaged tissue (Fig. 5c) as compared to the alignment shown in tissues healed without dressing (Fig. 5b). The higher magnification image clearly shows the hair follicle and hair growth after 9 days of post operation (Fig. 5d). Well organized epithelial cells and large number of collagen are obvious in higher magnification image of the growing wound healing area (Fig. 5e, f).

4 Conclusions

Chitosan scaffolds have been designed, modified and impregnated with antibiotic to fasten wound healing. Release study showed modified scaffold (cht/PEG) exhibits greater and faster drug release as compared to pure chitosan scaffold. Greater drug release has been confirmed through zone of inhibition and turbidity measurements. Biodegradation, swelling property and water vapour transmission rates have been measured and found the suitability of modified scaffold as better dressing material. In-vivo evaluation of scaffolds has been performed on mice; cell growth during healing process has been closely monitored and verified the faster healing process in modified scaffold vis-à-vis pure chitosan scaffold and control.

Acknowledgments The authors would like to thank the University Grant Commission, India for the financial support to carry out the work. The authors also wish to thank UGC-DAE-CSR, Indore for SEM, DSC and XRD measurements. Also, thanks to Mr. Sameer Gupta, SRF, Pineal Research Lab, Department of Zoology, Banaras Hindu University, Varanasi for helping in in vivo studies.

References

1. F.L. Mi, S.S. Shyu, Y.B. Wu, S.T. Lee, J.Y. Shyong, R.N. Huang, Biomaterials **22**, 165 (2001)
2. L.S. Nair, C.T. Laurencin, Prog. Polym. Sci. **32**, 762 (2007)
3. A.S. Hoffman, Adv. Drug. Deliver. Rev. **54**, 3 (2002)
4. R.C. Nagarwal, P.N. Singh, S. Kant, P. Maiti, J.K. Pandit, J. Control. Rel. **136**, 2 (2009)
5. J.H. Sung, M.R. Hwang, J.O. Kim, J.H. Lee, Y.I. Kim, J.H. Kim, S.W. Chang, S.G. Jin, J.A. Kim, W.S. Lyoo, S.S. Han, S.K. Ku, C.S. Yong, H.-G. Choi, Int. J. Pharm. **392**, 232 (2010)
6. C.M. Shih, Y.T. Shieh, Y.K. Twu, Carbohyd. Polym. **78**, 169 (2009)
7. S.K. Pandey, R.M. Banik, Bioresour. Technol. **102**, 4226 (2011)
8. P. Laurienzoa, M. Malinconico, A. Motta, A. Vicinanz, Carbohyd. Polym. **62**, 274 (2005)
9. A. Sionkowska, Polym. Degrad. Stabil. **91**, 305 (2006)
10. K. Madhumathi, P.T.S. Kumar, S. Abilash, V. Sreeja, H. Tamura, K. Manzoor, J. Mater. Sci. Mater. M **21**, 807 (2010)
11. K.G. Naber, B. Bergman, M.C. Bishop, Eur. Urol. **40**, 576 (2001)
12. B. Yang, X.Y. Li, S. Shi, X. Kong, G. Guo, M. Huang, F. Luo, Y. Wei, X. Zhao, Carbohyd. Polym. **80**, 860 (2010)
13. M. Sinha, P. Maiti, R.M. Banik, Int. J. Res. **2**, 72 (2011)
14. K. Kwangsok, K.L. Yen, C. Chang, D. Fang, B.S. Hsiao, B. Chu, M. Hadjiargyrou, J. Control. Rel. **98**, 47 (2004)
15. F. Chen, Z. Shi, K.G. Neoh, E.T. Kang, Biotechnol. Bioeng. **104**, 30 (2009)
16. S.L. Tomic, M.M. Mic, S.N. Dobic, J.M. Filipovic, E.H. Suljovrujic, Radiat. Phys. Chem. **79**, 643 (2010)
17. R.K. Dey, A.R. Ray, Biomaterials **24**, 2985 (2003)
18. M. Burkatovskaya, G.P. Tegos, E. Swietlik, T.N. Demidova, A.P. Castano, M.R. Hamblin, Biomaterials **27**, 4157 (2006)
19. B.M. Min, Y. You, J.M. Kim, S.J. Lee, W.H. Park, Carbohyd. Polym. **57**, 285 (2004)
20. F.G. Pearson, R.H. Marchessault, C.Y. Liang, J. Polym. Sci. **43**, 101 (1960)
21. M.M. Coleman, P.C. Painter, Prog. Polym. Sci. **20**, 1 (1995)
22. R. Jayakumar, R.L. Reis, J.F. Mano, J. Macromol. Sci., Pure Appl. Chem. **A44**, 271 (2007)
23. Q. Wang, J. Zhang, A. Wang, Carbohyd. Polym. **78**, 731 (2009)
24. H. Zhang, S.H. Neau, Biomaterials **22**, 1653 (2001)
25. M.L. Zhang, X.H. Gong, Y.D. Zhao, N.M. Zhang, Biomaterials **23**, 2641 (2002)
26. P. Wu, E.A. Nelson, W.H. Reid, C.V. Ruckley, J.D.S. Gaylor, Biomaterials **17**, 1373 (1996)
27. D. Shim, D.S. Wechsler, T.R. Lloyd, R.H. Beekman, Cardiovasc. Diagn. **39**, 287 (1996)
28. A. Song, A.A. Rane, K.L. Christman, Acta Biomater. **8**, 41 (2012)